



TOWN COUNCIL MINUTES

LEGISLATIVE HEARING

November 21, 2022 @ 5:15 p.m.

The Kure Beach Town Council held a Legislative Hearing on Monday, November 21, 2022 at 5:15 pm. The Town Attorney was present and there was a quorum of Council members present.

COUNCIL MEMBERS PRESENT

Mayor Craig Bloszinsky
MPT Allen Oliver
Commissioner John Ellen
Commissioner David Heglar

COUNCIL MEMBERS ABSENT

Commissioner Dennis Panicali

STAFF PRESENT

Town Clerk – Mandy Sanders
Deputy Town Clerk – Beth Chase

Mayor Bloszinsky called the meeting to order at 5:15 p.m. stating the purpose to receive comments on the proposed text amendment to the following section of the Kure Beach Code: Kure Beach Code: KBC 15.36.140 Roof Pitch

Official notice of this Legislative Hearing was posted on the Town's website and bulletin board on October 27, 2022 and was advertised in the Island Gazette on November 2, 2022 and November 9, 2022, thus meeting notification requirements.

MOTION- Commissioner Heglar made a motion to excuse Commissioner Panicali from the meeting

SECOND- Commissioner Ellen

VOTE- Unanimous

Mayor Bloszinsky opened the Legislative Hearing at 5:15 p.m.

Town Clerk Sanders read a letter received by a resident hereby incorporated into the minutes.

No other comments were received.

MOTION- Commissioner Ellen made a motion to close the Legislative Hearing at 5:19 p.m.

SECOND- MPT Oliver

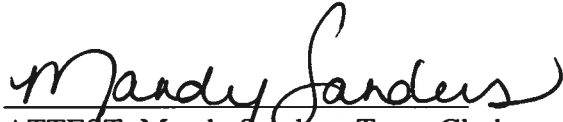
VOTE- Unanimous

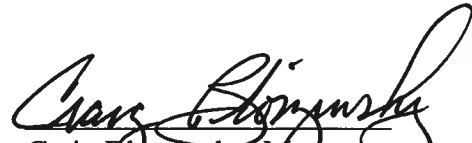


TOWN COUNCIL MINUTES

LEGISLATIVE HEARING

November 21, 2022 @ 5:15 p.m.


ATTEST: Mandy Sanders, Town Clerk


Craig Bloszinsky, Mayor

NOTE: These are action minutes reflecting items considered and actions taken by Council. These minutes are not a transcript of the meeting. A recording of the meeting is available on the town's website under government>council.

Beth Chase

From: Galbraith, Craig <galbraithc@uncw.edu>
Sent: Sunday, November 20, 2022 7:38 AM
To: Allen Oliver; David Heglar; Craig Bloszinsky; John Ellen; Dennis Panicali
Cc: Beth Chase; Mandy Sanders; James E. Eldridge; John Batson
Subject: Roof Pitch topic, 5:15pm legislative hearing
Attachments: Article 1 roof slope.pdf; Article 2 roof slope.pdf

Follow Up Flag: Follow up
Flag Status: Flagged

Dear Council Members

Tomorrow at 5:15pm the Council has a legislative hearing for comments of the roof pitch amendment to the KBC Code.

As Chairperson of the P&Z, I will represent officially the recommendation to approve this item (it was a 4-1 vote, I was the no vote). However, since this is an open hearing, I am now speaking as a resident (and owner of several houses in KB). However, I will not speak publicly at our meetings outside my role as Chairperson of the P&Z.

Thus, below is a message (with attachments) from an e-mail I sent the Mayor a month ago. I would like this entered into the record regarding this issue as a resident (not representing P&Z) regarding this issue. Thank you.

Dear Mayor

During the last P&Z meeting we discussed the roof issue as a design issue - as you know, I voted against the motion to recommend deleting this section in the Kure Beach code. It was my opinion that roof design is, in fact, a safety issue, and not a pure aesthetic design issue as per current NC State Statutes (which focuses on local governments ability to regulate aesthetics issues with residential buildings).

I have now had time to do a lot more research on this, and there are plenty of published peer review articles that clearly show roof design does influence roof failure in high winds due to pressure differences (attached two). But roof failure during a hurricane is also clearly a safety issue, since it can hurt people and property, both the owners and adjacent, and become more expensive/time consuming to clean up.

Most of these published studies looked at different types of gabled roofs. I could not find an article that specifically compared high wind damage to flat versus gabled roofs, but there are a number of studies to show flat roofs have more damage and failure in rainy areas than gabled roofs.

Bottom line is that I believe it is clear that roof design in our ordinances is NOT a pure design issue re State Statutes (which is not dealing with safety concerns, but rather aesthetic), but rather contains a safety component in Kure Beach due to the high winds and intense rain that we occasionally get (perhaps in Raleigh roof design doesn't matter, but in the Coastal Carolinas it is a safety issue also)

Due to this I strongly believe it is wrong to delete that part of the ordinance regarding roof design without further research. It might be appropriate to do additional research regarding if flat roofs are, indeed, more dangerous, but to eliminate the roofing design part of our local ordinance (given our lack of knowledge about this) due to the current State limitations re design I believe is completely wrong. Note that meeting code (flat roofs can meet code as do all the gabled roofs) does not reduce the Safety argument since many of the studies cited examined roofs that all met code, but still failed due to design differences.

Craig

Craig S. Galbraith, MBA, MSc, Ph.D., CPVA
Duke Progress Entergy/Betty Cameron Distinguished Professor
GlaxoSmithKline Scholar, Economic Development
Coordinator, Entrepreneurship minor program
Department of Management, Cameron School of Business
University of North Carolina Wilmington
910-962-3775, galbraithc@uncw.edu

A. Baskaran,¹ S. Molleti,² and D. Roodvoets³

Understanding Low-Sloped Roofs Under Hurricane Charley From Field to Practice

ABSTRACT: Natural wind hazard damages have been dramatic in recent years, incurring losses of life and property around the world. Wind-induced failure is one of the major contributors to insurance claims, and it is rising. To address these growing concerns, RICOWI (Roofing Industry Committee on Weather Issues) started a Wind Investigation Program (WIP) to investigate the field performance of roofing assemblies after major windstorm events and to factually describe roof assembly performance and modes of damage. As part of this program, Hurricane Charley, which hit Punta Gorda, FL, with winds exceeding 140 mph (63 m/s), was investigated. This paper mainly focuses on the field performance of the low-sloped roofs with three important parameters that were found critical in the failure of the roofing systems, namely, • Effect of corner wind suction, • Effect of parapet, • Effect of internal pressure. For each scenario, first scientific documentation was presented, and then how the field observation reflects the fundamental principles were discussed. Based on this exercise, correlations are developed for roof wind design. In addition, wind impact data from the North American codes of practice are also calculated and compared to show the impact of science and field observation on durable roof design. With these illustrations, this paper offers recommendations to advance the roof system design for hurricane-prone regions.

KEYWORDS: roofs, hurricanes, parapet, internal pressure, wind tunnel, dynamic test, wind loads

Introduction

Natural wind hazards such as typhoons and hurricanes have been dramatic in recent years, incurring losses of life and property damages. Figure 1 shows the trend of the damage amounts of the most costly hurricanes in the United States. As shown in Fig. 1 [1], the years 2004 and 2005 can be considered as the worst hurricane disaster years incurring total losses of 45 and 115 billion U.S. dollars respectively (not adjusted for inflation). Of these, Hurricane Charley, in the year 2004 was a Category 4 event (Categories

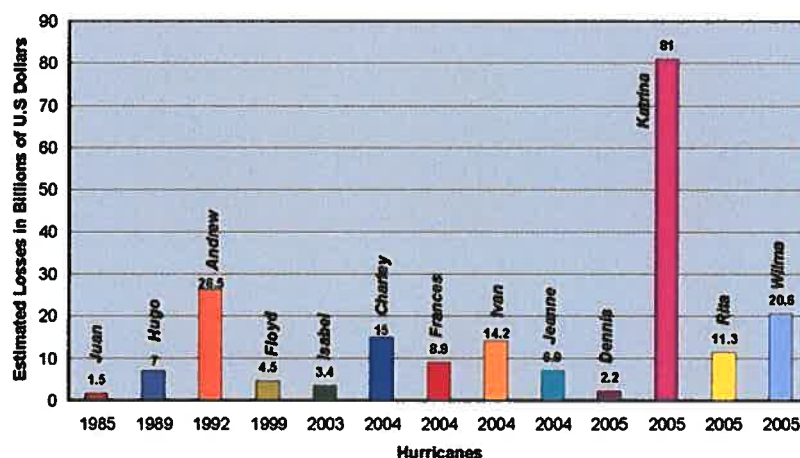


FIG. 1—Approximate cost of hurricanes (Source: NOAA).

Manuscript received February 9, 2007; accepted for publication October 8, 2007; published online October 2007. Presented at ASTM Symposium on Roofing Research and Standards Development: Sixth Symposium on 2 December 2007 in Tampa, FL; W. Rossiter and T. Wallace, Guest Editors.

¹ Vice-Chair, Senior Research Officer, Roofing Industry Committee on Weather Issues, National Research Council Canada, Ottawa, Ontario, Canada K1A 0R6. E-mail: bas.baskaran@nrc.ca.

² Research Officer, National Research Council Canada, Ottawa, Ontario, Canada K1A 0R6.

³ Ex Chair, Roofing Industry Committee on Weather Issues, 6710 Lakefront Dr., Montague, MI 49437.

range from 1–5 with 5 having the highest wind speeds and severe damage expected) incurring losses of 15 billion U.S. dollars across the areas of Florida and South Carolina. In contrast to Hurricane Katrina, where the damages were a combination of water and wind-induced failures, nearly all damages from Hurricane Charley were wind-induced failure. Wind-induced failure is one of the major contributors to insurance claims, and it is rising. Therefore, understanding how to prevent wind damages by establishing engineering standards or standard practices will allow designers to design roofs that can sustain high winds.

Hurricanes Hugo and Andrew created awareness of roof failures. There was also concern that the truth of the causes of failures, and the types of products that failed was distorted [2,3]. Following these storm events, two workshops were devoted to identify and discuss roof wind uplift issues and solutions [4]. One of the outcomes of these workshops resulted in the establishment of the Roofing Industry Committee on Weather Issues (RICOWI). An additional outcome was the formulation of the “Special Interest Group for Dynamic Evaluation of Roofing Assemblies” (SIGDERS), a North American roofing consortium.

RICOWI is made up of 15 sponsors representing the major roofing associations and 42 affiliates representing general interested parties. RICOWI started a Wind Investigation Program (WIP) with a mission:

1. To investigate the field performance of roofing assemblies after major wind storm events;
2. To factually describe roof assembly performance and modes of damage; and
3. To formally report the results for substantiated wind speeds.

Keys to the RICOWI investigations are that investigation teams are balanced, unbiased, and trained in wind damage assessment. The teams typically are made up of a manufacturer, a roofing consultant, university or insurance organization personnel, and a manufacturer from another part of the roofing industry. Initial training for the investigation teams occurred at Oak Ridge National Lab (ORNL) in 1996 [4]. Training focused on how winds interact with the built environment, how to detect wind damage, wind direction, and causes of the damage. Badges were issued to each member of the team that attended the training seminar. Attendance was mandatory for the issue of badges (official U.S. Department of Energy badges) which members used for identification purposes during the wind investigation.

In the year 2004, Hurricane Charley, with winds exceeding 140 mph (63-m/s) made landfall with a direct hit on Punta Gorda, FL. WIP deployment criteria is 95 mph (43-m/s) sustained winds. Based on this, field investigation started after it was determined that the storm had the appropriate wind and sufficient roof damage. A small scouting team that reported back to RICOWI headquarters made this effort. Within the first week after the storm, the teams were called out and assembled, and arriving on site the teams were updated on the storm’s extent and other issues such as safety and communication measures.

All inspections documented the investigations using standard forms, and the failure modes were photographed. At the end of each day of investigation reports were completed and were provided to the administrator, and also a feedback session occurred so that the teams could follow up on interesting leads. Although teams typically worked from the highest wind-damaged areas to the less wind-damaged areas, there was no attempt to get randomized data. Towards the end of the investigation report the writers that were members of the investigation teams developed a final report from the data [5]. This paper mainly focuses on the field performance of the low-sloped roofs as discovered in the investigations after Charley.

The objective of this paper is not to present several photographs and information related to specific roof configurations. Rather, efforts were made to scrutinize all these photographs and field observations towards developing a relationship with the existing science in the wind and roofing field. In doing so, and to respect the page limitation of the paper, only three important parameters that were found critical in the failure of the roofing systems are selected, namely,

1. Effect of corner wind suction
2. Effect of parapet
3. Effect of Internal pressure

For each scenario, first scientific documentation was presented, and then how the field observation reflects the fundamental principles are discussed. Based on this exercise, correlations are developed for roof wind design. In addition, wind design data from the North American codes of practice are also calculated and compared to show the impact of science and field observation on durable roof design. With these illustrations, this paper offers recommendations to advance the roof system design for hurricane-prone regions.

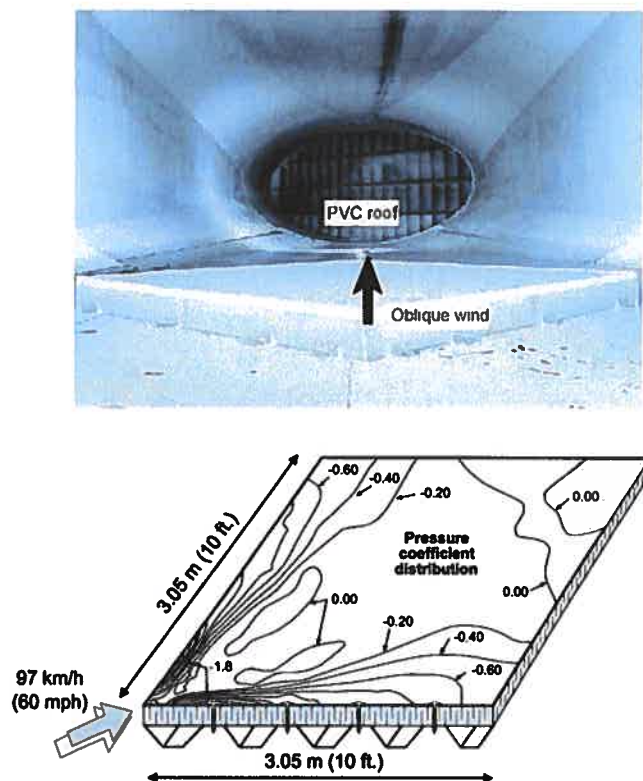


FIG. 2—Wind tunnel model and wind-induced pressure distribution over a roof assembly [6].

Correlation of Field Failure Observations with the Existing Knowledge

Effect of Corner Wind Suction

Wind flow around buildings creates both negative and positive fluctuations over a roofing system. The negative pressure is created by the flow separation on the windward side of the roof, while the positive pressure is created by the internal pressure in the building. The internal positive pressure is dependent on the location of dominant openings in the building and it is generated by the wind flow into the building and the temperature difference across the envelope. These pressures are dynamic and can be separated into static and fluctuating components. The static component is simply the mean pressure. The transient component occurs as a random process and its dominant frequencies depend on the frequency of the upstream wind and the geometry of the building. Thus the wind effect on roofing and its response is dynamic.

As mentioned before, wind pressure distribution varies spatially over a roof and it can have high suction at the corner and perimeter, due to vortex flow and separations. This science is clearly displayed in Fig. 2, which represents pressure variation on a building roof taken from a wind tunnel study at National Research Council of Canada (NRC) [6]. The wind tunnel tests were carried out in the 30-ft by 30-ft (9-m by 9-m) NRC wind tunnel. These tests used full-scale roofing components 10-ft by 10-ft (3 by 3-m in size) having different heights. For wind directions perpendicular to a building face (normal wind) and at 45 degrees to a face (oblique wind) measurements were made in smooth wind and turbulent wind conditions for five wind speeds, ranging from 30 to 60 mph (13.4-m/s to 26.8-m/s). As shown in Fig. 2, a PVC (polyvinyl chloride) roofing system was tested with 81 pressure taps fitted on the single-ply membrane to measure the unsteady pressure loads on the roof [6]. In total, 30 configurations were tested in this wind tunnel study. Wind-induced corner suctions are evident from Fig. 2 with maximum measured mean pressure coefficient (C_p) of 1.8 on corners. Pressure coefficients (C_p) are the nondimensional ratios of wind-induced pressures on a building to the dynamic pressure (velocity pressure) of the wind at the reference height, which is the roof eave height.

Case Study 1: Failure Investigation of a School Roof—Figure 3 shows the failure investigation of a school roof in which the above-discussed scientific data have been correlated to the field observation. All the photographs shown in Fig. 3 are taken from the top of the roof under investigation. P1 shows the

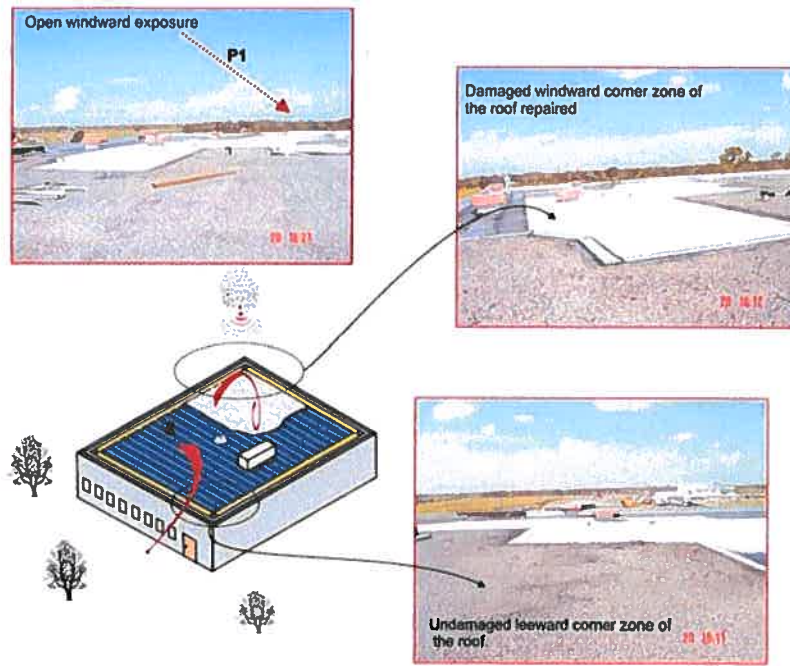


FIG. 3—Roof assembly failure due to high suctions caused by cornering wind (not to scale).

prevailing windward exposure condition. According to the American codes standards of practice [7], this can be classified as Exposure C whereas the Canadian building code [8] classifies it as open country exposure. Even though there is variation in the terminologies, both of them define that “open terrain with scattered obstruction having flat open country, grasslands and water surface as the criteria for this exposure condition.”

The building under investigation was a 40-ft (12-m) high concrete-walled gymnasium. It is part of a school used as a shelter during Hurricane Charley, although it was not designated as a shelter. The building is of substantial construction with concrete walls and a lightweight concrete deck. There was only one exterior fire escape door that led to the outside. It was reported as closed during the storm. Primary access was through the corridors of the adjacent building. The entire complex with several roof areas totaled more than 140 000-ft² (13 000-m²). The damaged roof area section was about 40 000-ft² (3700-m²) and had a stone surface four-ply BUR (built-up roofing). The membrane was attached to a lightweight concrete deck mechanical fastener. A large section of the gymnasium roof (over 40 % of the membrane) blew off during the storm when about 400 people were inside. This released a large volume of water that spread across most of the school complex. Other than some limited edge metal damage, there was no damage to about 100 000-ft² (9300-m²) of roof on adjacent parts of the structure. These sections were all BUR membrane roofs appearing to be of the same construction as the sections that were blown off.

The gymnasium roof structure did not appear to fail because of pressurization below the deck; the cause appears to have been purely suction force. The school roof was the highest point in several miles, so it took the brunt of the hurricane’s force. The low 2-ft (0.7-m) parapet in the upwind corner did not help to reduce the maximum uplift (also refer to discussion of Figs. 4 and 5). The roof failure pattern was typical of the uplift forces that would be present in a cornering wind with an L-shaped area. As temporary repairs had been made, it was not possible to determine the sequence of failure. It is interesting to correlate the failure shape with the wind pressure distribution diagram of Fig. 2 where the roof corner experiences high suction. This was the similar phenomenon in the case of the school roof, where those high suction pressures on the corner of the roof caused the failure of the roof.

Effect of Parapet

Most low-sloped roofs have a parapet. It is the low wall built along one side of, or, all around the perimeter of a low-sloped roof, where it may modify the wind flow over the roof so that the pressure on it is more uniformly distributed. It also provides a measure of safety in that no objects (gravel, for example) are so easily blown into the street below. Parapets have been of research interest from the early 1970s and several

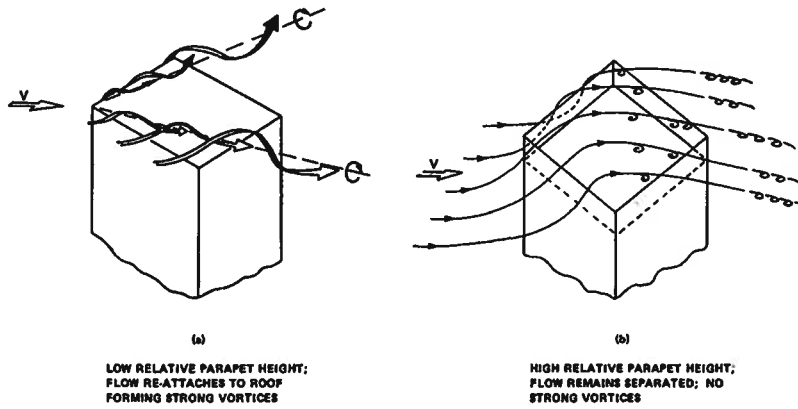


FIG. 4—Effect of parapet height on wind flow over roofs [19].

wind studies are being carried out to quantify the influence of a parapet on roof wind loads [9–14]. Figure 4 shows a typical wind flow over roofs with parapet. According to Kind et al. [15–19], increased parapet height generally resulted in more favorable pressure distributions. That is, maximum suctions were reduced and suction peaks were broadened so that pressures are less nonuniform and monotonic, there was no “worst” nonzero parapet height. Parapets are also effective in preventing stone blow-off from the buildings having ballasted roof systems. However, limitations do exist regarding the effectiveness of the parapet height in providing resistance to the phenomenon of stone blow-off [15,20]. Field observation on a gravel roof with a low parapet confirms these scientific theories (Fig. 5).



FIG. 5—Wind vortex formation on gravel roofs due to low parapet.

Building standards and codes only recently provided guidelines in the context of parapet effects on wind-induced suction pressures on low-sloped roofs. The effect of perimetric parapets on pressure coefficients differs from one region of a roof to another:

- Generally the mean pressure coefficients at the field region of the roof have minimum effect by parapets. Therefore, one may assume wind loads for field regions of roofs are the same regardless of the existence of a parapet.
- At the edge regions, parapets decrease the peak pressure coefficients. A low parapet, i.e., a parapet less than 3-ft (1-m) high, reduces these pressure coefficients by up to 10 % for tall [60-ft (20-m) or higher] buildings, and by up to 30 % for low [less than 60-ft (20-m) high] buildings. A high parapet reduces the peak pressure coefficients by up to 20 % for tall buildings, and by up to 15 % for low buildings. Overall, for the edge region, parapets are beneficial in reducing the suctions irrespective of the building and parapet heights.
- At corner regions (Fig. 6), low parapets tend to increase both the mean and peak pressure coefficients. In fact, with winds approaching a roof obliquely (at 45°), 1 to 1.2-ft (0.3 to 0.4-m) high parapets can roughly double the pressure coefficients at the corner regions of a roof of both low and tall buildings. Parapets of 3-ft (1-m) or higher, however, reduce the pressure coefficients of roof corners of tall buildings significantly, but only marginally on low buildings.

Based on the wind tunnel measurements, building codes recommend reduction in roof wind uplift design loads for tall buildings. Refer to Figs. I-9, I-15 and Figs. 6.11 and 6.17, respectively in the NBCC [8] and ASCE 7 [7].

Case Study 2: Success Story of Condominium Building—Figure 7 shows the beneficial effect of a parapet on the wind uplift resistance of a roof assembly. The investigated building was a six-story condominium building, stucco wall construction with a poured concrete roof deck. Granule surface BUR system was over mopped-in-place with perlite insulation. Roof was approximately 37 000 ft² (3400 m²). The perimetric parapets were designed well and the field measurements indicated they are about 5-ft (1.5-m) high. Parapet corners are also well designed and capped with a single piece of metal coping. Wind-related damages were limited to approximately 5 % of the wall/parapet cap and the underside of the soffit. No damages were observed to the roof. As shown in the photograph of Fig. 7, the building is relatively new and exposed to waterfront exposure (“Exposure C”—ASCE 7 [7], “Open terrain”—NBCC [8]). This exposure condition is considered to be the most severe exposure condition. As illustrated in Fig. 6, due to high perimetric parapet configuration, the wind suctions on the rooftop of the condominium might have reduced, which possibly could have caused fewer damages to the roof assembly. Also there were many individual HVAC units that were mounted on the condominium rooftop stands and all of these were in excellent condition. No movement was apparent for any of the HVAC units. However, the surrounding buildings in the neighborhood of this condominium, which had no parapets, experienced severe damages. One such building with gravel blow-off from the roof is also shown in Fig. 7. This gravel blow-off exposed the membrane to the ultraviolet radiation which may eventually reduce the durability of the roof assembly. Note that the parapet is not the only important factor for the roof assembly to sustain hurricane force uplift. Parapets with sufficient height can influence in reducing the wind-induced loads. It is equally important that other good roofing practices such as attachment of the assembly (i.e., adhesion, cohesion, mechanical attachment, air barrier, etc.) should be adequate to sustain whatever uplift forces it experiences. Failure to do so can blow off the roof whether a sufficient height parapet is present or not.

Case Study 3: Success Story of Commercial Building—Figure 8 presents a success story of a commercial building roof assembly, which might have survived due to the high parapet. Roof area was approximately 5 000 ft² (460 m²) with a 5.5-ft (1.8-m) parapet on the storefront side, a 4.5-ft (1.5-m) shared wall on one side, a 3-ft (1-m) parapet on the third side, and a gutter edge along the rear side. Granule surface modified bituminous membrane was installed directly over mechanically attached insulation, which had metal deck as the substrate. No damages were noticed on the roof assembly. However, contrary to Case Study 2, there were several blow-offs of HVAC (heating ventilation and air conditioning) panels. More severely, some of the air-handling units lifted from their base due to the lack of proper attachment. It has also been observed that these units moved in distance from the base as far as the electric wiring allowed. These blow-offs and flip-flop movements caused punctures of the roof membrane and resulted in the failure of the waterproofing capacity of the roof assembly.

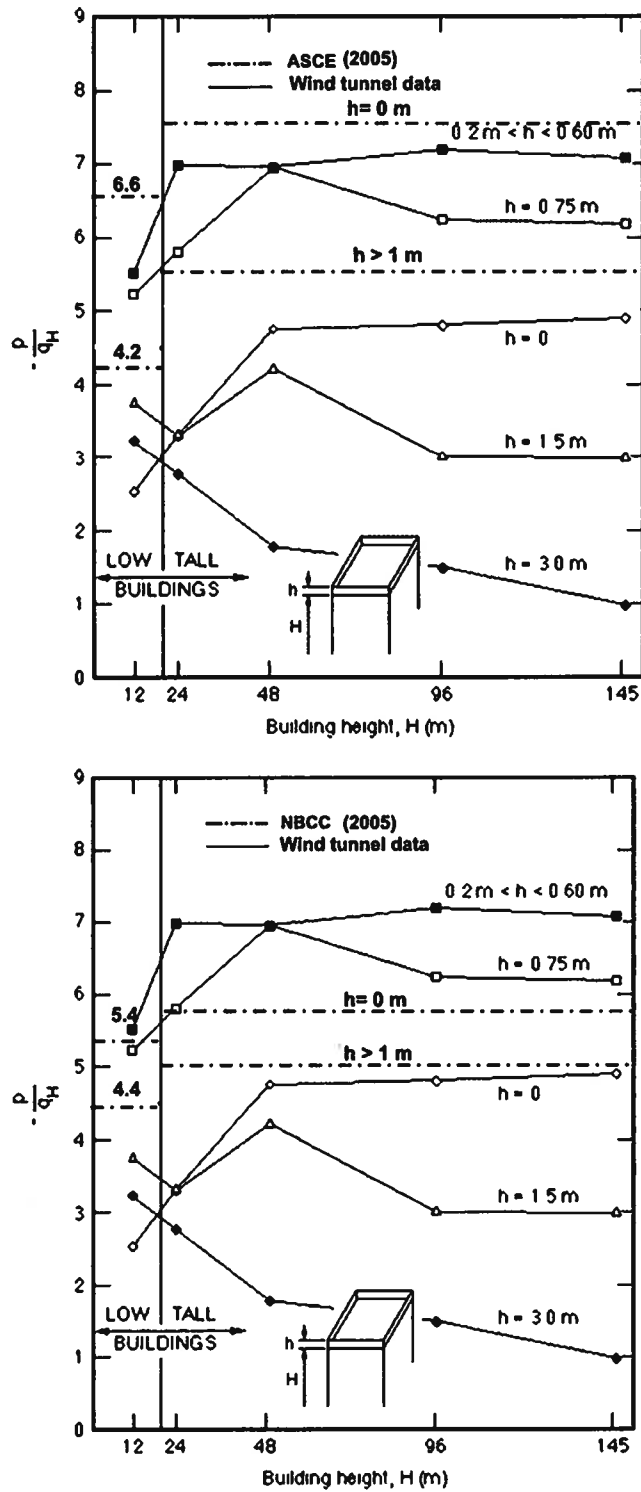


FIG. 6—Relationship of code specifications (NBCC [8] and ASCE [7]) to measured data [9] regarding pressure coefficients on roof corners with parapet.

Recommendation from Field to Practice

Corner wind can cause high wind suction and the use of a high parapet can mitigate those high suction. Wind flow aerodynamics over a roof area has been modified based on the presence of a parapet and its height. These modifications affect the wind-induced suction on the roof assembly. Measured data show that high parapets on a tall building show a beneficial effect in suction reduction. Therefore, in hurricane-prone regions use of parapets over 3-ft (1-m) high are recommended.

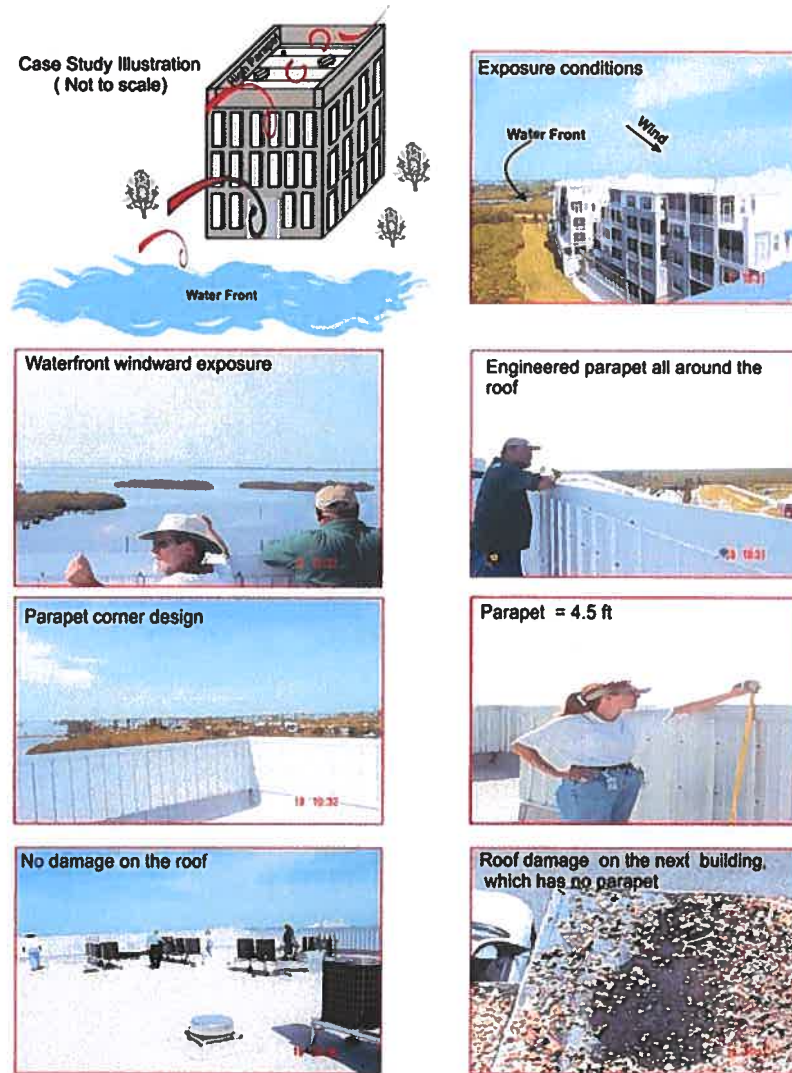


FIG. 7—Beneficial effect of parapet on the wind uplift resistance of a roof system.

Effect of Internal Pressure

Design wind pressure on a roof is the algebraic sum of the external pressure and internal pressure across the roof assembly. It can be presented as follows:

$$p = I_w q (C_e C_g C_p - C_e C_{gi} C_{pi}) \text{ lbf/ft}^2 \quad (1)$$

$$p = 0.00256 K_z K_{zt} K_d V^2 I (GC_p - GC_i) \text{ lbf/ft}^2 \quad (2)$$

$C_e C_{gi} C_{pi}$ and GC_i are the internal pressure components, respectively, according to NBCC [8] and ASCE [7]. The magnitudes of these internal coefficients depend on the distribution of the openings and air leakage paths in the building envelope. Due to the uncertainties of the size and distribution of openings in the building, the internal pressure coefficients can have a wide range as given below:

NBCC: Openings Category

- Category 1: C_{pi} : -0.15 to 0.0
- Category 2: C_{pi} : -0.45 to 0.3
- Category 3: C_{pi} : -0.7 to 0.7

ASCE: Enclosure Classification

- Open Buildings: GC_i : 0.00
- Enclosed Buildings: GC_i : +0.18, -0.18
- Partially Enclosed Buildings: GC_i : +0.55, -0.55

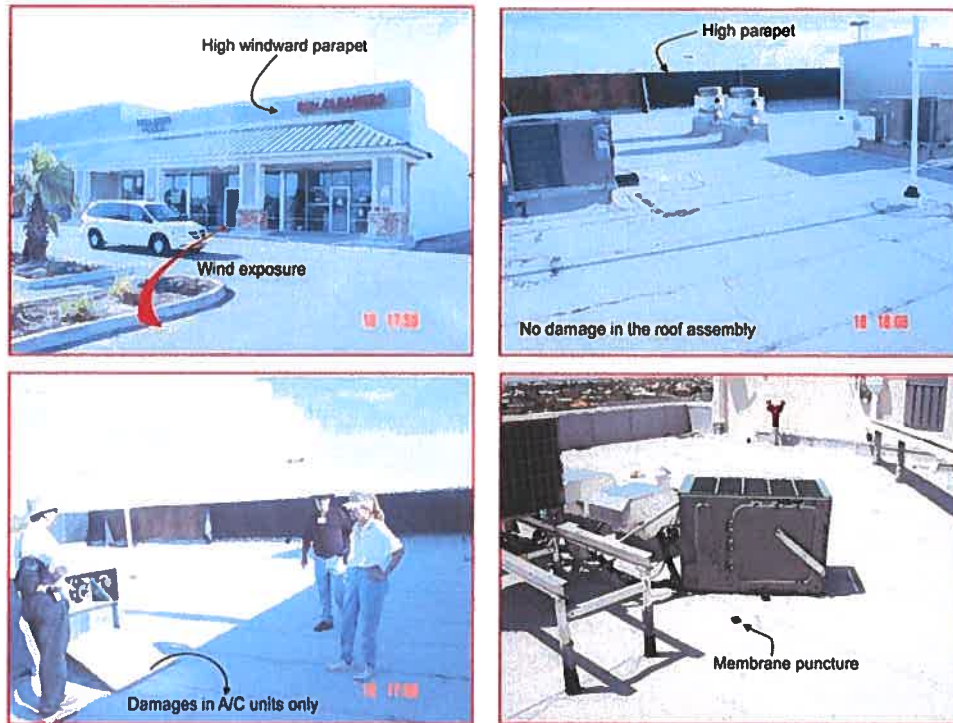


FIG. 8—Survived roof assembly due to high parapet and damages caused by the rooftop equipments.

Examples of Wind Load Calculation With/Without Internal Pressure—Two buildings of height 30-ft (10-m) and 70-ft (21-m) are located in a hurricane-prone region having a wind speed of 150 mph (67-m/s). These buildings have an importance category II and exposure conditions of C. With the assumption of building “enclosed” before a storm and building becomes “partially enclosed” during the storm, Table 1 illustrates the variation of design pressures using ASCE 7 [7]. Similar calculations are performed using NBCC [8] for the same building located in the high wind region of Newfoundland and the results are also presented in Table 1.

With the assumption that the 30-ft (10-m) low-rise building was designed and constructed as an enclosed building, the design pressures as per ASCE 7 [7] indicated in Table 1 are 67, 112, 168 lbf/ft² (3.2, 5.4, 8 kPa) for the field, edge, and corner, respectively. Now, during the hurricane with winds blowing at a speed of 150 mph (67-m/s), assume that the low-rise building undergoes deformation of

TABLE 1—Variation in design pressure with the respect to the internal pressure.

ASCE				
Roof Zone	Low-Rise Building		High-Rise Building	
	Enclosed psf	Partially Enclosed psf	Enclosed psf	Partially Enclosed psf
Field	67	88	107	131
Edge	112	133	167	192
Corner	168	189	227	252
NBCC				
Roof Zone	Low-Rise Building		High-Rise Building	
	Category 1 psf	Category 3 psf	Category 1 psf	Category 3 psf
Field	32	53	52	78
Edge	44	66	79	104
Corner	96	117	120	146

Note: 1 psf=47.88 Pa.

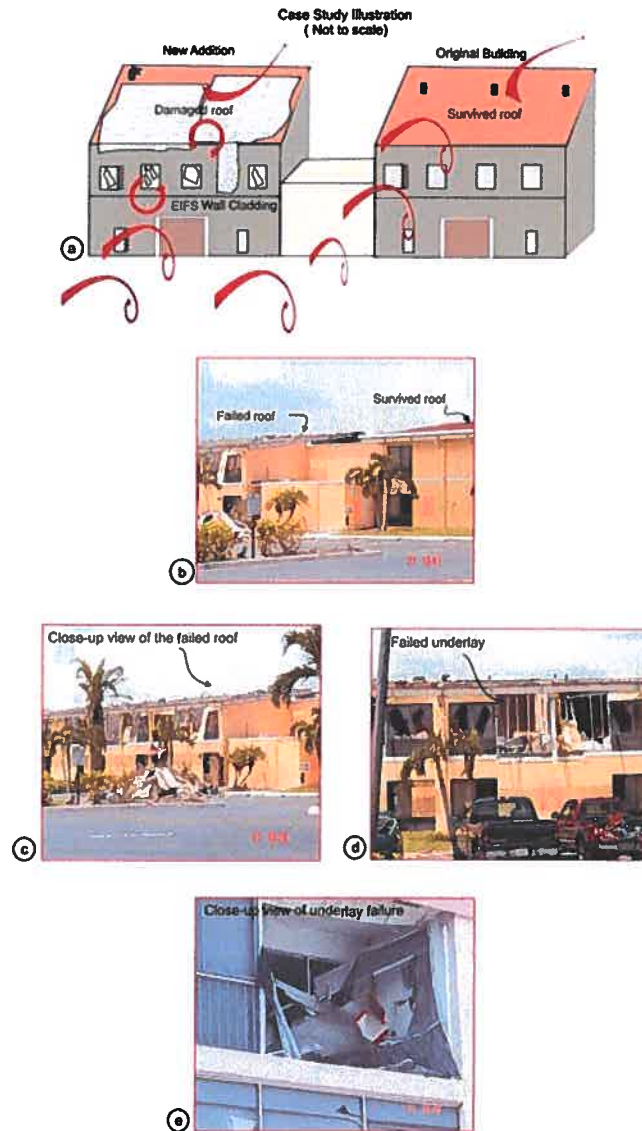


FIG. 9—(a–e) Roofing assembly failure due to sudden build-up in the internal pressure.

walls and damages to the windows, making the building partially enclosed. The design pressures for the roof covering will be increased as illustrated in Table 1 as 88, 133, 189 lbf/ft² (4.2, 6.4, 9 kPa) for the field, edge, and corner, respectively. The transition from enclosed to partially enclosed has resulted in an increase of design pressure by 21 lbf/ft² (1 kPa) for the three zones of the roof. A similar trend was also observed in the design pressures of the low-rise building calculated using NBCC [8]. This increase in the design pressure indicates that for the buildings located in the hurricane-prone regions or high-wind regions, the roof design should account for these high probability situations that could occur from the severity of the storm. It should be noted that this 21 lbf/ft² (1 kPa) increase is only on the design pressures and not on the required resistance of the roof assembly. In order to obtain the required resistance, the design pressures are to be multiplied by appropriate safety factors. Systems tested under dynamic testing can use a value of 1.5 as a safety factor (CSA [21]) whereas statically tested systems can use a safety factor of 2.0 or higher. In other words, for this particular low-rise building, the roof covering should be designed as a partially enclosed building with design pressures of 88, 133, 189 lbf/ft² (4.2, 6.4, 9 kPa) for the field, edge, and corner, respectively, and the required resistance should be 176, 266, and 378 lbf/ft² (8.4, 12.7, 18 kPa), respectively. The following case study will clearly illustrate how the transition from an enclosed building to a partially enclosed during Hurricane Charley led to failure of the roof and it signifies the pivotal role of internal pressure on the roof covering design.

Case Study 4: Failure Investigation of a Multi-Occupancy Building—As shown in Fig. 9, the failed

roof assembly belongs to a multi-occupancy building. The building is comprised of two sections, the section on the right was an old construction on which the roof survived. An addition to this section on the left was a relatively new construction on which the roof assembly completely failed. The walls of this new addition were constructed of EIFS (Exterior Insulation and Finish System). Field failure observation indicated poor integration of wall/window interface. In other words, windows were just plastered without any anchorage to the structural support to the walls as part of the whole building envelope system. As a result, the blowing wind on the windward side, as shown in Fig. 9, ripped apart the windows from the EIFS, surged inside the building and increased the internal pressure, which ultimately lifted the entire roof assembly. In contrast, the old construction was of brick cladding and the windows were properly integrated with the building envelope, and as shown in Fig. 9, it was devoid of any damage. This case study is a good illustration of the scientific phenomenon of internal pressure build-up and the severity of the damage it can cause to the roof assembly.

Recommendation from Field to Practice

Internal pressure build-up can increase the roof failure probability. Probabilities of window cladding failures are high in hurricane-prone regions and such failures can significantly increase the internal pressure that can lead to roof uplift failures. It is recommended that the designer should allow provisions to account for such failures during the design and the selection of the roofing system. This can be achieved by classifying the building as Category 3 as per NBCC [8] or partially enclosed building as per ASCE 7 [7].

Need for Engineered Edge Design

Perimeters and corners of low-sloped roofs have been recognized as the most vulnerable areas of the roof. The high uplift found in these areas has been factored into the model national buildings codes, and resisting these loads has been a requirement of the codes for many years. Failure, however, continues to occur at these vulnerable parts of buildings because both design and installation practices are inadequate. The negative forces at the perimeter must be resisted by adequate mechanical attachment or bonding of the roofing membrane to the substrate and deck. Many designs allow pressurization of the underside of the roofing system, which significantly adds to the loads that must be resisted. The load to be resisted is dynamic and most tests used to evaluate roofing systems are static, or quasistatic. Tests also focus on the vertical force of uplift, but the forces, once they break the initial bond or mechanical attachment become peel forces that are not measured in current testing. In current testing the first mechanical failure (screw withdrawal) or separation of the membrane stops the test. In nature roofs survived with small amounts of initial failure if the peel forces were resisted. If the peel forces are resisted catastrophic damage is less likely.

Prior to 2004 there were no code requirements for roof edge attachment. This has been corrected with the addition of ANSI/SPRI/ES-1 [22] Edge Design Standard For Low-Sloped Roofs as a code requirement in the International Building Code. This illustrates the point, however, that building codes prefer to reference consensus standards as the basis for design and installation requirements. This is where ASTM (American Society for Testing and Materials) and other standards developers must be working to understand the problems and develop tests and standard practices that provide more pertinent data and functional systems.

Conclusions

This paper presented the relationship between field observations during Hurricane Charley and the existing science in the wind engineering and roofing field. This has been discussed for three important parameters that were found critical in the failure of the roofing systems, namely,

- Effect of corner wind suction
- Effect of parapet
- Effect of internal pressure

In each of these scenarios, first, scientific documentation was presented, and then how the field observation

reflects the fundamental principles was discussed. Wind design data from the North American codes of practice are also calculated and presented to show the impact of science and field observation on durable roof design.

Acknowledgments

The presented research is being carried out for a consortium, the Special Interest Group for Dynamic Evaluation of Roofing Systems (SIGDERS) formed from a group of partners interested in roofing design. These partners included:

Manufacturers: Atlas Roofing Corporation, Canadian General Tower Ltd., Carlisle Syn Tec., GAF Materials Corporation, GenFlex Roofing Systems, Firestone Building Products Co., IKO Industries Ltd., ITW Buildex, Johns Manville, Sarnafil Roofing, Soprema Canada, Stevens Roofing, Tremco and Trufast.

Building Owners: Canada Post Corporation, Department of National Defence, Public Works and Government Services Canada.

Industry Associations: Canadian Roofing Contractors' Association, Canadian Sheet Steel Building Institute, National Roofing Contractors' Association and Roof Consultants Institute.

The authors would like to acknowledge the contribution of the following members of the field investigation team: Helen Hardy-Pierce, GAF Materials Corporation, Kenneth R. Hunt, Performance Roofing Systems Inc., Ron Kough, GAF Materials Corporation, and Stan Houston, FEMA.

References

- [1] National Oceanic and Atmospheric Administration (NOAA), "The Deadliest, Costliest, and Most Intense United States Tropical Cyclones from 1851 to 2006 (and other frequently requested hurricane facts)," Technical memorandum, NWS TPC-5, April 2007.
- [2] Cook, R. A. and Soltani, M., "Hurricanes of 1992—Lessons Learned," *Proceedings of Symposium by American Society of Civil Engineers*, Dec. 1–3, 1993.
- [3] Smith, T. L., Kind, R. J., and McDonald, J. R., "Hurricane Hugo: Evaluation of Wind Performance and Wind Design Guidelines for Aggregate Ballasted Single-Ply Membrane Roof Systems," *Proceedings of the VIII International Roofing and Waterproofing Congress*, 1992, p. 598.
- [4] Baskaran, B. A., Desjariais, A., Roodvoets, D., and Wood-Shields, P., "Strategic Plan for the Wind Event Investigation Program," *8th U.S. Wind Engineering Conference*, Baltimore, MD, June 1997, pp. 1–5.
- [5] RICOWI (Roofing Industry Committee on Weather Issues), Hurricanes Charley and Ivan Wind Investigation Report, RICOWI Inc., Powder Springs, GA, 2006.
- [6] Savage, M. G., Baskaran, A., Cooper, K. R., and Lei, W., "Pressure Distribution Data Measured During the November 1994 Wind Tunnel Tests on a Mechanically-Attached, PVC Single-Ply Roofing System," IAR Report LTR-A-003, National Research Council, Canada, 1996.
- [7] American Society of Civil Engineers, Standard ASCE 7-2005, "Minimum Design Loads For Buildings and Other Structures," 2005.
- [8] NRC (National Research Council), National Building Code of Canada, Part 5. Ottawa: National Research Council of Canada, Ottawa, Ontario, Canada, K1A 0R6, 2005.
- [9] Baskaran, A., "Wind Loads on Flat Roofs With and Without Parapets," M.Eng. thesis, Concordia University, Montreal, 1986.
- [10] Baskaran, A. and Stathopoulos, T., "Roof Corner Wind Loads and Parapet Configuration," *J. Wind. Eng. Ind. Aerodyn.*, Vol. 29, 1988, pp. 79–88.
- [11] Kopp, G., Surry, D., and Mans, C., "Wind Effects of Parapets on Low Buildings: Part 1. Basic Aerodynamics and Local Loads," *J. Wind. Eng. Ind. Aerodyn.*, Vol. 93, No. 11, 2005, pp. 817–841.
- [12] Kopp, G., Mans, C., and Surry, D., "Wind Effects of Parapets on Low Buildings: Part 2. Structural Loads," *J. Wind. Eng. Ind. Aerodyn.*, Vol. 93, 2005, pp. 843–855.

- [13] Kopp, G., Mans, C., and Surry, D., "Wind Effects of Parapets on Low Buildings: Part 3. Parapet Loads," *J. Wind. Eng. Ind. Aerodyn.*, Vol. 93, 2005, pp. 857–872.
- [14] Kopp, G., Mans, C., and Surry, D., "Wind Effects of Parapets on Low Buildings: Part 4. Mitigation of Corner Loads with Alternative Geometries," *J. Wind. Eng. Ind. Aerodyn.*, Vol. 93, No. 11, 2005, pp. 873–888.
- [15] Kind, R. J. and Wardlaw, R. L., "The Development of a Procedure for the Design of Rooftops Against Gravel Blow-Off and Scour in High Winds," *Proceedings of the Symposium on Roofing Technology*, 1977, p. 112.
- [16] Kind, R. J. and Wardlaw, R. L., "Wind Tunnel Tests on Loose-Laid Roofing Systems for Flat Roofs," *Proceedings of the Second International Symposium on Roofing Technology*, 1985, p. 230.
- [17] Kind, R. J., Savage, M. G., and Wardlaw, R. L., "Further Model Studies of the Wind Resistance of Two Loose-Laid Roof Systems (High-Rise Buildings)," National Research Council of Canada, Report LTR-LA-269, April 1984.
- [18] Kind, R. J., Savage, M. G., and Wardlaw, R. L., "Further Wind Tunnel Tests of Loose-Laid Roofing Systems," National Research Council of Canada, Report LTR-LA-294, April 1987.
- [19] Kind, R. J., Savage, M. G., and Wardlaw, R. L., "Pressure Distribution Data Measured During the September 1986 Wind Tunnel Tests on Loose-Laid Roofing Systems," September 1987.
- [20] SPRI (Single Ply Roofing Industry), RP-4, "Wind Design Standard for Ballasted Single Ply Roofing Systems," 2002.
- [21] CSA Number A123.21-04, "Standard Test Method for the Dynamic Wind Uplift Resistance of Mechanically Attached Membrane-Roofing Systems," Canadian Standards Association, Canada, 2004.
- [22] SPRI (Single Ply Roofing Industry) ES-1 "Wind Design Standard for Edge Systems Used with Low Slope Roofing Systems," Needham, MA, 2003.



Variations of wind pressure on hip roofs with roof pitch

Y.L. Xu^{a,*}, G.F. Reardon^b

^a *Department of Civil and Structural Engineering, The Hong Kong Polytechnic University,
Hung Hom, Kowloon, Hong Kong, China*

^b *Cyclone Testing Station, Department of Civil and Systems Engineering,
James Cook University of North Queensland, Townsville, Qld 4811, Australia*

Received 29 July 1996; revised 21 February 1997; accepted 22 September 1997

Abstract

Three hip roofed building models of 15°, 20°, and 30° roof pitch, respectively, are tested in a wind tunnel to investigate wind pressure distributions over hip roofs and the effect of roof pitch on roof pressures. The pressures measured on the hip roofs are then compared with those on gable roofs of otherwise similar geometry to evaluate the effect of roof shape on roof pressures. Finally, the measured roof pressures of commonly-used probability of occurrence are compared with Meecham's work in terms of local mean and peak pressures. The results show that roof pitch does affect both the magnitude and distribution of hip roof pressures. The 30° hip roof experiences the highest peak suction at roof corner among the three tested hip roofs. The worst peak suctions are much smaller on the hip roofs than on the gable roofs for 15° and 20° roof pitches. However, the worst peak suctions on the hip and gable roofs are almost the same for 30° roof pitch. It is also seen that the magnitudes and distributions of local mean and peak pressures on the low pitched hip roof tested here are compatible with the results from Meecham's work on a hip roof of similar geometry. © 1998 Elsevier Science B.V. All rights reserved.

Keywords: Roof pressure; Roof pitch; Hip roof; Gable roof; Comparative study

1. Introduction

It has been long recognised that roof geometry used in houses and low-rise buildings may significantly influence wind pressures on the roof due to the change in the flow patterns around the houses and buildings. Extensive wind tunnel studies carried out by Davenport et al. [1] and Holmes [2] have led to important conclusions regarding the effect of roof slope upon wind pressures of low-rise buildings with a gable roof. As several post disaster investigations on wind-induced damage to

* Corresponding author. E-mail: ceylxu@polyu.edu.hk.

building roofs revealed that hip roofs had better performance than gable roofs during severe cyclones [3,4]. Sparks et al. [5] measured mean wind pressures on both gable and hip roofs in a wind tunnel with the aim of predicting the risk of structural damage associated with roof shape. Meecham et al. [6] also carried out a comparative study of the magnitude and distribution of both mean and peak pressures between a gable roof and a hip roof, and related them to the structural framing of each type of roofs. They found that the worst peak pressure on the hip roof was reduced by as much as 50% from that on the gable roof. The finding, however, was based on one roof pitch of 18.4° only. It is not known yet if the finding still applies for other roof pitches and if roof slope affects wind pressure on hip roof in a similar way to gable roof. This situation has led structural and architectural professionals to express concern at the lack of knowledge of the wind pressures on hip roofs. They now have to estimate wind pressures on hip roofs based on their own judgement.

This paper, therefore, presents a wind tunnel study of wind pressures over hip roofs and their variations with roof pitch. The wind pressures measured on the hip roofs are compared, whenever possible, with those on the gable roofs studied by Holmes [7] and well known to most structural and architectural professionals. The measured roof pressures of commonly-used probability of occurrence are finally compared with Meecham's work [6] on a hip roof to have a cross-check of experimental results and measurement conditions.

The present study, however, is only a preliminary study on hip roofed buildings with emphasis on the understanding of hip roof pressures, through a comparison with well-known gable roof pressures, to facilitate both quasi-static and fatigue designs of roof claddings and their connections. Correspondingly, only point roof pressures were measured in this study. The average roof pressures over a roof panel were not considered because the actual size of roof panel varies very much around the two hip slopes and because the average roof pressures on the gable roofs are not available in Holmes's work [7] for conducting a reasonable comparison. The wind forces on the supporting structural system and foundation of a hip roofed building were not included either in this study. However, there is no doubt that further studies on average wind pressures over hip roofs together with other factors, such as effects of terrain category and aspect ratios of wall length to width and to height, are required.

2. Experimental technique

The experiments were carried out at the James Cook University Boundary Wind Tunnel. The wind tunnel has been described previously by Holmes in detail [8]. Briefly, it is of open-circuit configuration with an axial-flow fan mounted downwind of the working section. The working section was 17.5 m long, 2.5 m wide, and 2.0 m high.

A 1 : 50 scale model of natural wind was developed in the tunnel to simulate the natural wind over open-country terrain. The flow simulation technique mainly consisted of mounting a 400 mm high single plain fence spanning the floor at the start of the test section and covering the whole working section with low-pile carpet. The mean

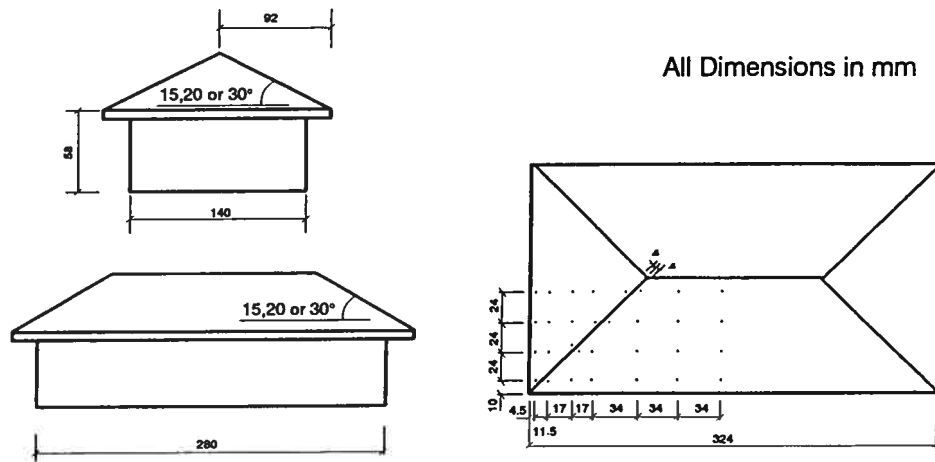


Fig. 1. Model configurations and pressure tap locations.

longitudinal wind speed profile measured in the tunnel was in good agreement with the power law of an exponent of 0.14. The mean wind speed was 10.1 m/s and the longitudinal turbulence was 0.2 measured at the 58 mm height of the wall of the building models. At a 78 mm height in the wind tunnel, the measured integral length of longitudinal turbulence was approximately 40 m in full scale. Compared with the full-scale integral length from the von-Karman spectrum at the same terrain [9], there was a small distortion of a factor of 1.27 in the scale of turbulence.

Three building models with hip roofs of 15°, 20°, and 30° roof pitch and large overhangs were made at a geometric scale of 1 : 50 (see Fig. 1). The selected roof pitches and large overhangs are commonly used in the houses and low-rise buildings with hip roofs in Australia. The aspect ratio (wall length to wall width) of the building models was chosen as 2 : 1. The height of the wall was 58 mm for all the three building models. Except for roof shape, the dimensions of the three hip roof building models chosen here were the same as those of the three gable roof building models tested by Holmes in the same wind tunnel [7]. Therefore, a good comparison of wind pressures can be made between the gable roofs and hip roofs.

In consideration of the symmetric conditions of the building models, a total of 31 taps were arranged on only a quarter of each roof. Each building model was tested at a 10° increment from 0° to 360° and at additional directions of 45°, 135°, 225°, and 315°. Particular attention was paid to the number and position of the taps near hip ridge, roof edge, and roof ridge, from which the air flow is probably separated to form a region of high velocity gradients and high local turbulence and vorticity. Fig. 1 shows the basic model configurations and pressure tap locations on the hip roofs.

The building models were constructed from 6 mm thick “perspex” sheet. The pressure taps of 10 mm long pieces of 1.6 external diameter and 1.0 mm internal diameter stainless-steel tubing were inserted into the holes drilled in the “perspex”, with one end of the tubing flush with the roof surface. Pressure measurements were

carried out using two Honeywell 163 pressure transducers mounted within 48 port “Scanivalves”. The pressure taps on the model were connected to the “Scanivalves” by 450 mm long pieces of 1.6 mm internal diameter vinyl tubing with two 0.3 mm internal diameter restricters placed along the tubing. This pressure measurement system gave a linear frequency response up to 100 Hz and a gradual attenuation from 100 Hz to about 300 Hz with a “half power” point. The reference velocity was taken at the 58 mm height during all experimental runs, measured by a hot-film mounted about 0.5 m side and 0.5 m upwind of the model, and used to calculate pressure coefficients. The static pressure was taken from the static holes of a pitot static tube mounted at 1 m above the floor during each run and was then converted to the static pressure at the 58 mm height in terms of a profile of static pressure measured through the boundary layer of the wind tunnel. The static pressure at 58 mm height was only slightly smaller than that at 1 m height. The signals from the transducers were low-pass filtered at 250 Hz and were digitally sampled using a Data 6000 analyser. The sampling frequency was 1000 Hz and the sampling duration of each run was 32 s.

For each run, wind pressures measured on the models were expressed in the form of a non-dimensional pressure coefficient, defined as follows:

$$C_p(t) = \frac{p(t) - p_0}{\frac{1}{2}\rho U^2}, \quad (1)$$

where p_0 is the static pressure at the reference height of 58 mm, U the mean longitudinal wind speed at the reference height and ρ the air density.

The mean pressure coefficient ($C_{P_{\text{mean}}}$), root mean square (rms) pressure coefficient ($C_{P_{\text{rms}}}$), minimum and maximum pressure coefficients ($C_{P_{\text{max}}}$ and $C_{P_{\text{min}}}$) were calculated from each pressure coefficient record. The average values of five records are presented mainly for the comparative study with Holmes’ work on the gable roofs whilst the highest negative peak pressure in the five records for each tap on each hip roof is used essentially for the comparative study with Meecham’s work on the hip roof. The total measurement time for the almost continuous five records is about 160 s. This corresponds to from 32 to 65 min in full scale depending on design wind speeds and design philosophy [10]. Hence, the measured highest negative peak pressures from the five records possess the commonly-used probability of occurrence.

3. Mean pressures

3.1. Mean pressures at 0°, 45°, and 90°

Fig. 2a–2c, show the spatial distributions of mean wind pressure coefficient measured on the three hip roofs and averaged from the five records for wind directions, 0°, 45°, and 90°, respectively. The symmetric conditions have been considered in plotting these figures from the test data.

In the 0° wind direction, all mean wind pressures are negative for the 15° and 20° pitch roofs. Nevertheless, for the 30° pitch roof some positive mean wind pressures

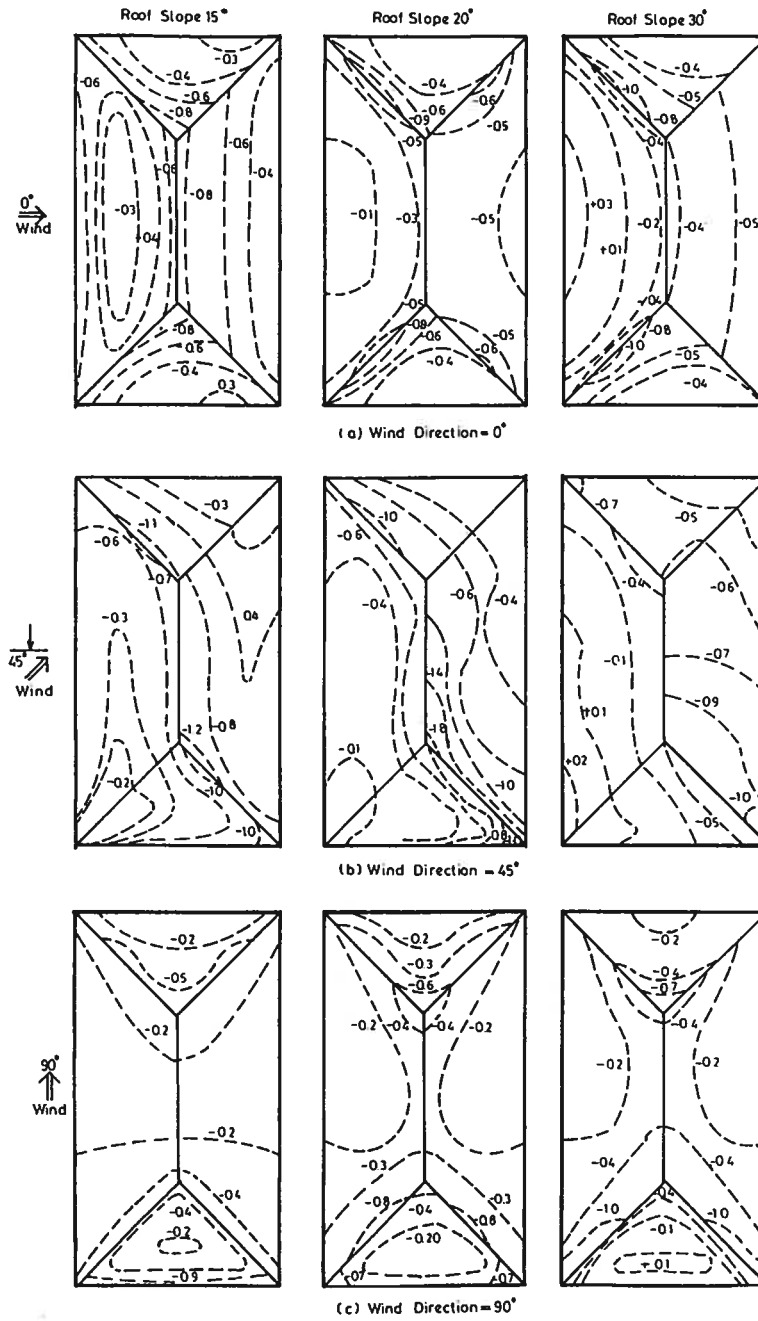


Fig. 2. Mean pressure coefficient distributions over three hip roofs. (a) Wind Direction: 0°, (b) 45°, and (c) 90°.

appear on the windward slope, but on the leeward slope and two side slopes mean wind pressures are still negative. High mean suctions on the 15° pitch roof occur in the band near the leeward roof ridge and around the area immediately behind the windward hip ridges. The occurrence of these high mean suctions is believed to be caused by the separation bubbles downwind of the leading edges. With the increase of roof pitch, the mean suctions become relatively uniformly distributed over the leeward roof slope. The mean suctions, however, significantly decrease on the windward roof slope and moderately increase on the two side roof slopes. For both 20° and 30° pitch roofs, high mean suctions occur in the area just behind the windward hip ridge. For the three roofs in the 0° wind direction, the 30° pitch roof experiences the highest mean suction in the area just behind the windward hip ridge with a mean wind pressure coefficient of -1.0 . The aforementioned mean wind pressure distributions clearly demonstrate that the effect of roof pitch on mean wind pressures over hip roof is considerable.

Mean wind pressure distributions on the three hip roofs in the 45° wind direction are totally different from those in the 0° wind direction (see Fig. 2a, Fig. 2b). The hip ridges parallel to the wind direction are no longer the places generating a thin but growing shear layer of high local turbulence and vorticity. The whole roof can be, therefore, seen as two parts, i.e., the windward slope (windward roof slope and side slope) and leeward slope (leeward roof slope and side slope). On either windward slope or leeward slope, the mean pressure contours are almost continuing across the hip ridges parallel to the wind direction. High mean suctions appear in the area immediately behind the roof ridge and the two hip ridges which are normal to the wind direction. For the concerned three hip roofs, the highest mean suction occurs on the 20° hip roof in a small area just behind the junction between the roof ridge and the hip ridge normal to the wind direction. The corresponding mean wind pressure coefficient is -1.8 , showing that much high suction occurs when wind direction is 45° compared with the wind direction of 0°. Compared with other hip roofs in the 45° wind direction, the 30° hip roof experiences relatively small mean suctions in the area behind the two hip ridges normal to the wind direction. This may be due to the high roof pitch generating the large size separation bubbles. Positive mean pressures also occupy almost half windward slope of the 30° hip roof.

For a gable roof, when wind direction is 90°, there is little effect of roof pitch on mean roof pressure, because the gable roof effectively presents a zero pitch to the wind [2]. For the hip roof, however, the effect of roof pitch on roof pressure is considerable. As shown in Fig. 2c, for the 15° hip roof pitch all mean wind pressures are negative with the leading eaves edge experiencing the highest mean suctions of -0.9 . For the 20° hip roof pitch, the highest mean suctions occur in the area just behind the windward hip ridges as well as the two front roof corners. For the 30° roof pitch, positive mean wind pressures appear near the leading eaves edge. The area behind the windward hip ridges close to the roof corners experience the highest mean suctions. Nevertheless, mean wind pressures are relatively uniformly distributed over most of the two side slopes along the long wall of the building for all the three hip roofs. The highest mean suction in this wind direction is -1.0 on the 30 pitch roof at the roof corners downwind of the front hip ridges.

In summary, the effect of roof pitch on mean wind pressure is significant for the hip roof. For the 0° wind direction, the highest mean suction occurs on the 30° pitch roof in the area just behind the windward hip ridges. The corresponding mean wind pressure coefficient is -1.0 . For the 45° wind direction, the area at the junction between the hip ridge and the roof ridge on the 20° hip roof experiences the highest mean suction with a mean wind pressure coefficient of -1.8 . For the 90° wind direction, the highest mean suction appears on the 30° hip roof in the area behind the hip ridges close to the roof corners with a mean pressure coefficient of -1.0 .

3.2. Comparison with Holmes' work

In 1981, Holmes carried out a comprehensive wind tunnel study of wind pressures on gable roofs. He tested three gable roof building models of 15° , 20° , and 30° roof pitch, respectively. Apart from roof shape, the basic dimensions of the three gable roof building models were the same as those of the three hip roof building models used in this study. Only point roof pressures were provided in his reports [2,7]. The sampling frequency and duration of each run used in his study was 500 Hz and 16 s, respectively.

Fig. 3a and Fig. 3b show his results on the spatial distributions of mean roof pressures over the three gable roofs for 0° and 90° wind directions, respectively [2]. Similar contours are not available for wind direction of 45° in his report [2]. Compared with Fig. 2a and Fig. 2c, it is seen that the mean pressure magnitudes and distributions on the gable roofs are quite different from those on the hip roofs, except for the 0° wind direction where the mean pressures around the middle part of the roofs are similar to each other. The results published in his report [7] showed that the highest mean suction occurred on the 15° pitch roof in the area just behind the roof ridge close to the gable end. The highest mean wind pressure coefficient was -1.0 . For the 45° wind direction, the small area near the gable end/roof ridge junction on the 20° roof pitch experienced the highest mean suction with a mean pressure coefficient of -2.73 . For the 90° wind direction, the highest mean suction occurred along the leading eaves edges with a mean pressure coefficient about -1.33 for all the three roofs. Compared with the hip roofs, the highest mean suction on the gable roofs are greater in the wind directions of 45° and 90° but the same in the wind direction of 0° .

3.3. Worst negative mean pressures

Although the contours of the worst negative mean pressure coefficients irrespective of wind direction cannot be directly used in design, the comparison of them with the contours of the worst fluctuating and peak pressure coefficients independent of wind direction can enhance our understanding of wind pressures on hip roofs.

Fig. 4 shows the contours of the maximum mean suction of each tap among all wind directions over the three hip roofs of 15° , 20° and 30° . For the 15° hip roof pitch, the worst mean suction is about -1.3 , distributing over the area near the roof ridge, the upper hip ridge, and the roof corner. For the 20° hip roof pitch, the worst negative

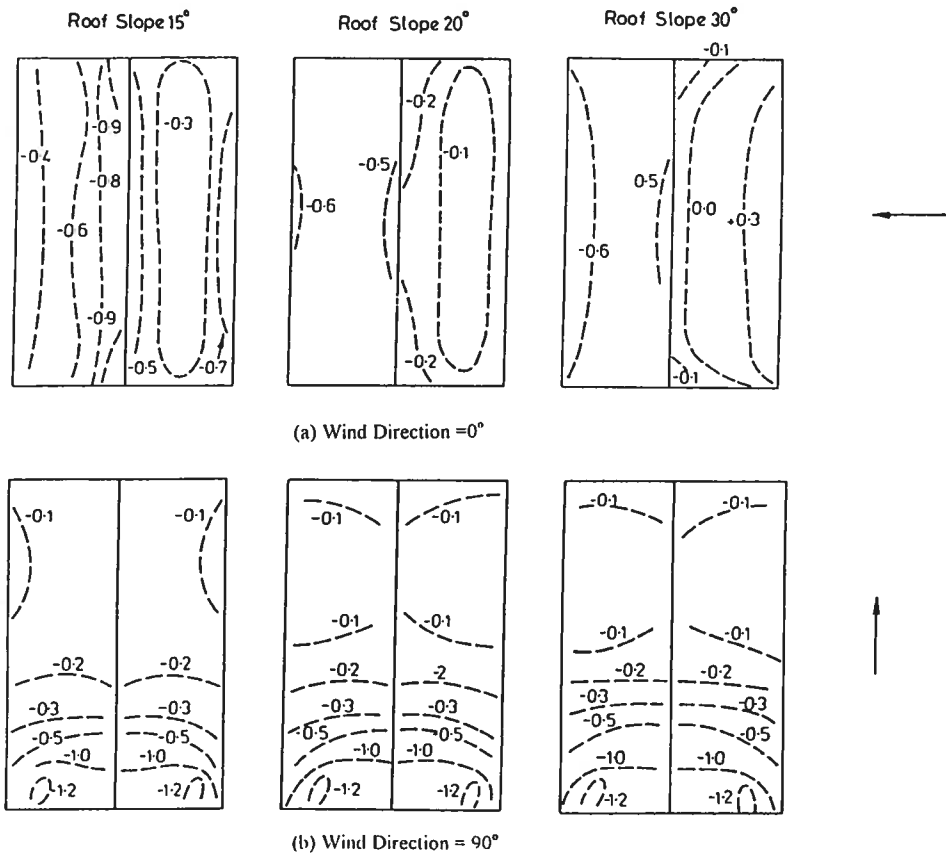


Fig. 3. Mean pressure coefficient distributions over three gable roofs (Holmes [2]). Wind direction: (a) 0° and (b) 90° .

mean pressure coefficient is about -1.8 , occurring at the area near the junction between the roof ridge and the hip ridge. For the 30° pitch roof, the roof corner experiences the worst mean suction with a -2.0 mean pressure coefficient. Having checked the wind directions causing these worst mean suctions, one may conclude that it is the separation bubbles downwind of the leading edge that cause high wind suctions. The worst mean suction contours are not given in the literature [2,7], and therefore no comparison is attempted to be made.

4. Fluctuating pressures

The fluctuating level of wind pressures occurring at a particular point and for a particular wind direction can be estimated by the rms pressure coefficient. The

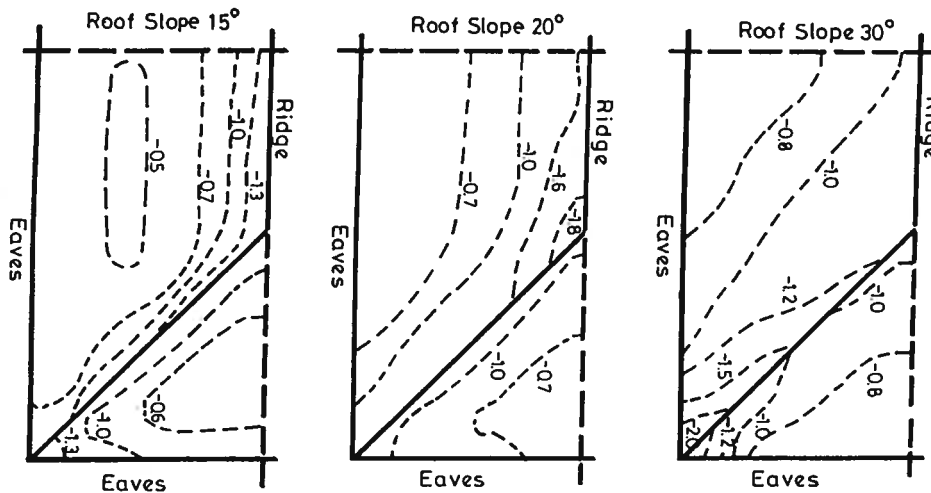


Fig. 4. Worst negative mean pressure coefficients independent of wind direction.

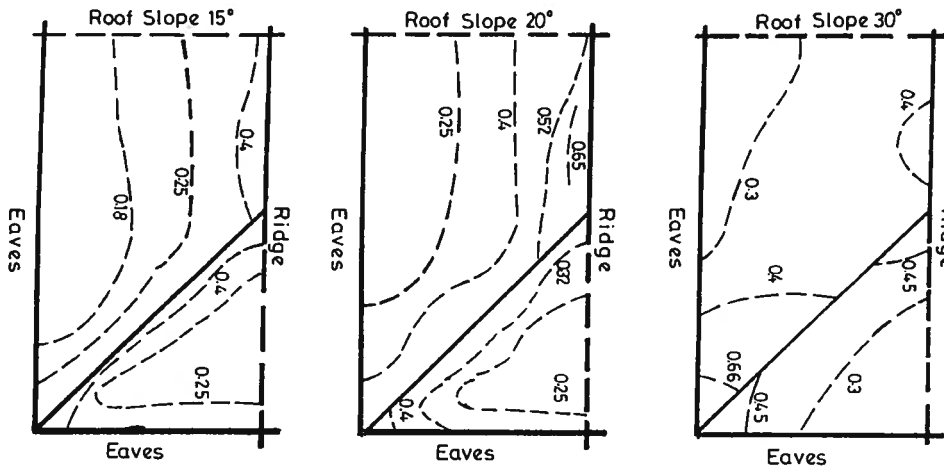


Fig. 5. Worst rms pressure coefficients independent of wind direction.

numerical value of the rms pressure coefficient depends on wind direction, the position of pressure tap over the roof, and roof pitch. For the 0° wind direction, high values of the rms pressure coefficients of 0.3 to 0.4 appeared in the area just behind the windward hip ridges for all three roofs. For the 45° wind direction, the 20° hip roof experienced the highest fluctuating pressure at a point near the roof ridge/hip ridge junction with a rms pressure coefficient of 0.65. For the 90° wind direction, the 30° hip roof underwent the highest fluctuating pressure at a point near the roof corner with a rms pressure coefficient of 0.63.

Fig. 5 shows the contours of the worst rms pressure coefficient irrespective of wind direction on the three hip roofs. It is interesting to see that the areas over which the

worst rms pressures distribute are almost the same as the worst negative mean pressures shown in Fig. 4. For the 15° hip roof pitch, the worst rms pressures distribute over the areas near the roof ridge, the hip ridge, and the roof corner of a coefficient of 0.4. For the 20° hip roof pitch, the worst rms pressure coefficient is about 0.65, occurring at the area near the roof ridge and upper hip ridge. For the 30° pitch roof, the roof corner experiences the worst rms pressures of a coefficient of 0.66.

5. Peak pressures

The distribution of the minimum peak pressure averaged from the five records for each tap over each roof was studied for the three wind directions. For the 0° wind direction, the minimum peak pressures of the highest magnitude took place in the area

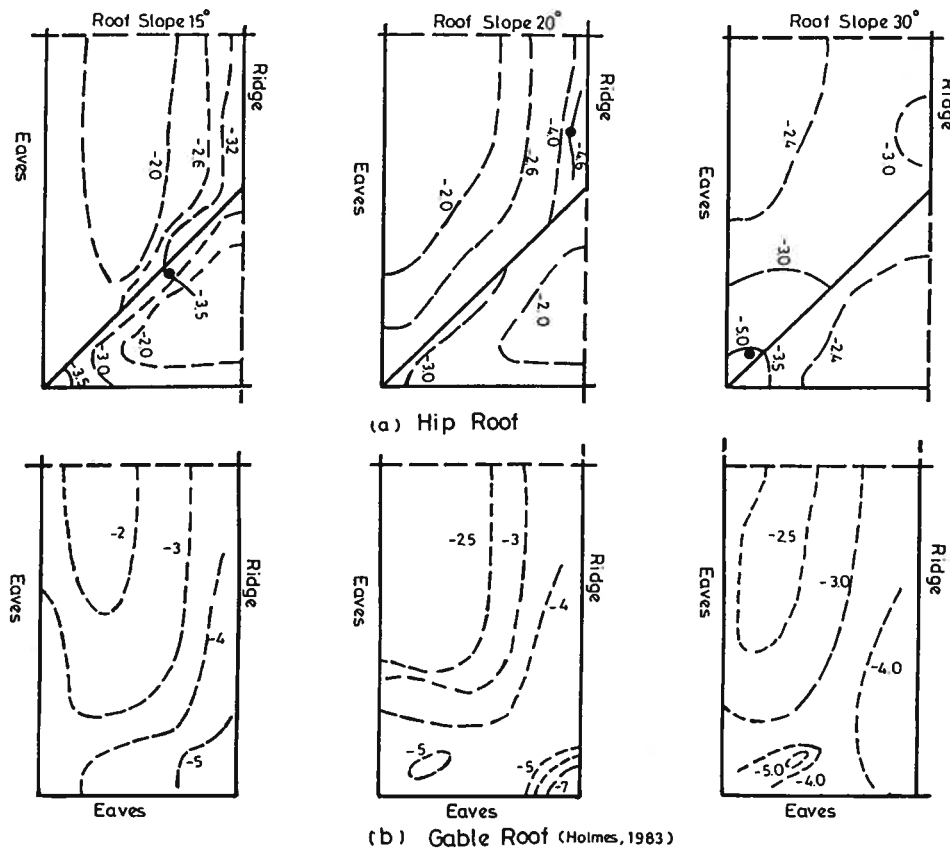


Fig. 6. Comparison of worst negative peak pressure coefficients independent of wind direction: (a) hip roof and (b) gable roof (Holmes [2]).

immediately behind the windward hip ridges for all three roof pitches. For the 45° wind direction, the minimum peak pressures of the highest magnitude also occurred in the area just behind the windward hip ridges normal to the wind direction and close to the roof ridge in the case of the 20° hip roof and close to the roof corner in the case of the 30° hip roof. When the wind direction is 90° , the minimum peak pressures of the highest magnitude were present at the windward roof corners for the 15° and 20° pitched roofs, but at the leeward roof corner for the 30° pitched roof.

The contours of the worst peak suction of each tap for all wind directions are shown in Fig. 6a for each hip roof. Fig. 6b shows the same quantity but for the gable roofs presented by Holmes [2]. For the 15° pitched roof, the hip ridge on the downwind side is the worst loaded region for the hip roof, but for the gable roof the roof ridge near the gable end is the worst loaded region. The largest minimum peak pressure coefficient among all taps for all wind directions is about -5.0 for the gable roof but only -3.5 for the hip roof. For the 20° pitched roof, the roof ridge near the hip ridge is the worst loaded region for the hip roof, and for the gable roof the worst area is at the junction between the roof ridge and the gable end. The largest minimum peak coefficient for the gable roof is about -7.2 but for the hip roof is only -4.6 . For the 30° pitched roof, the worst loaded region is the roof corner for both hip roof and gable roof, and the largest minimum peak coefficients are almost the same for the two types of roofs with a value about -5.0 . Therefore, it can be expected that for the 15° and 20° pitched roofs, the hip roof cladding will have better performance than the gable roof cladding during strong winds, but it may not be true for the 30° pitched roof.

It is interesting to note that the contour patterns of the worst negative peak pressures irrespective of wind direction are similar to those of the worst negative mean pressures independent of wind direction shown in Fig. 4. This indicates that the largest magnitude peak pressures are associated with the largest magnitude mean pressures, particularly within separation bubble regions.

6. Characteristics of pressures at critical taps

It has been mentioned in the last section that for each hip roof, there is a critical tap where the largest peak suction occurs among all the taps and for all the wind directions. The position of the critical tap actually varies with roof pitch, as marked in Fig. 6a. It is therefore interesting to see if the three critical pressures are actually excited under the same mechanism. Their probability distributions and spectral density functions are hence presented in this section after the introduction of variations of the pressures at the critical taps with wind direction.

Fig. 7a–7c show the variations of the four wind pressure coefficients at the critical taps with wind angle of attack for the 15° , 20° , and 30° hip pitched roof, respectively. From these figures, the critical wind directions in which the largest peak suction occur can be identified. The critical wind direction is 310° for the 15° hip roof, 135° for the 20° hip roof, and 120° for the 30° hip roof. Associating these critical wind

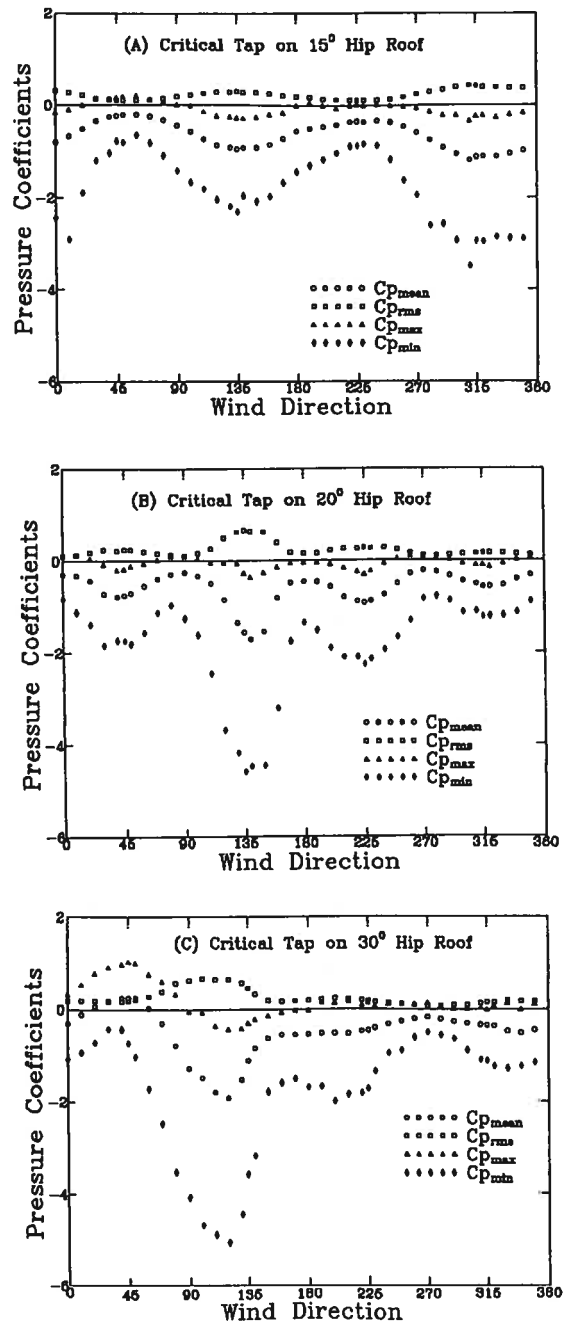


Fig. 7. Variation of pressure coefficients with wind direction.

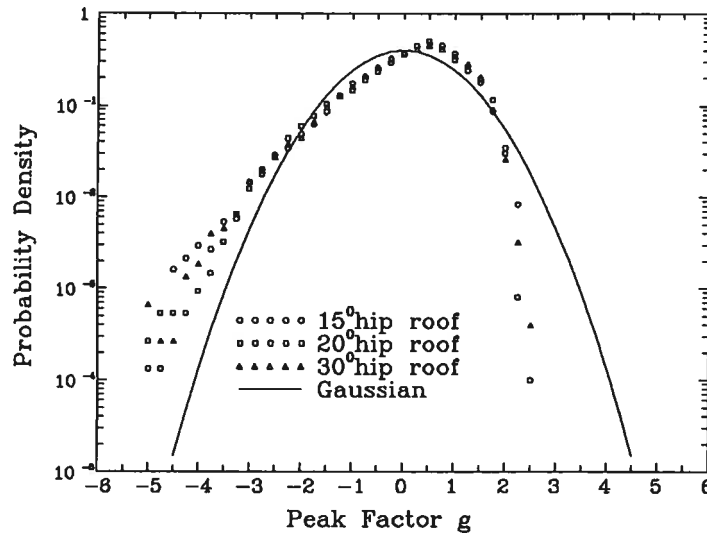


Fig. 8. Probability density functions of critical pressures.

directions with the leading edges of hip roofs, one can conclude that the separation bubbles downwind of leading edges cause the largest peak suctions. Fig. 7b and Fig. 7c also show that the occurrence of the largest peak suction is sensitive to wind direction for the 20° or 30° hip roof. That is, when wind direction slightly deviates from the critical wind direction, the peak suction reduces rapidly. It can also be seen from these figures that for the concerned three critical taps, the largest peak suctions are almost accompanied by the largest mean suctions and the largest fluctuations (rms).

To show the probability distributions of the pressures at the three critical taps, wind pressures are normalised as g using the following expression,

$$g(t) = \frac{p(t) - p_m}{p_{rms}} = \frac{C_p(t) - C_{p\text{ mean}}}{C_{p\text{ rms}}} \quad (2)$$

Extreme values of g correspond to maximum or minimum instantaneous pressures registered over the length of the measured record and are characteristic of wind pressure probability distributions.

Fig. 8 shows the probability distributions for the three critical pressures and the standard Gaussian density function. It is obvious that the probability distributions of the three critical pressures do not follow a Gaussian distribution. There are moderate deviations from the Gaussian distribution on both tails, which indicates a higher probability for the larger negative pressures and a lower probability for the larger positive pressures than a Gaussian density function would predict. The peaks of the measured functions are also shifted slightly to the positive side compared with the Gaussian density function. All three critical pressures possess a similar distribution

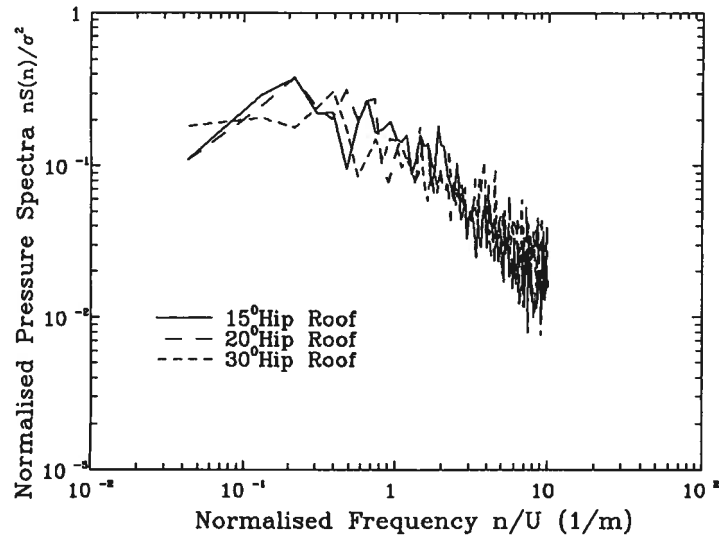


Fig. 9. Wind pressure spectra at critical taps.

which is common for negative wind pressures caused by separation bubbles. However, if compared with some taps at the roof corner of a gable building [11], the deviations of probability distribution from the Gaussian function for the three critical taps are much smaller, which indicates that the hip roof corner configuration may be able to prevent the occurrence of very high suction at roof corners.

The normalised spectra for the three critical pressures are shown in Fig. 9. The cut-off frequency is about 100 Hz. All the pressure spectra are broad band, i.e., significant fluctuating energy distributions over a broad frequency range. The three spectra are also similar to each other, giving an indication that all the three critical taps may be under the wind excitation of same mechanism.

7. Comparison with Meecham's work

Meecham et al. have reported their wind tunnel investigation of wind pressures and forces on a hip roofed building [6]. The geometric scale of the building model was 1 : 100 with a roof pitch of 18.4° and tested in both open country and suburban terrains. The aspect ratio of the building (length to width) and the eaves height were similar to the buildings in this study. However, there were no overhangs in their building model, and the sampling frequency and duration were not reported. The pressure coefficients they presented were referenced to the mean wind speed at mid-roof height.

Fig. 10 shows their contours of mean pressure coefficient over the hip roof for wind directions of 0°, 45°, and 90°, respectively. Compared with the contours of same

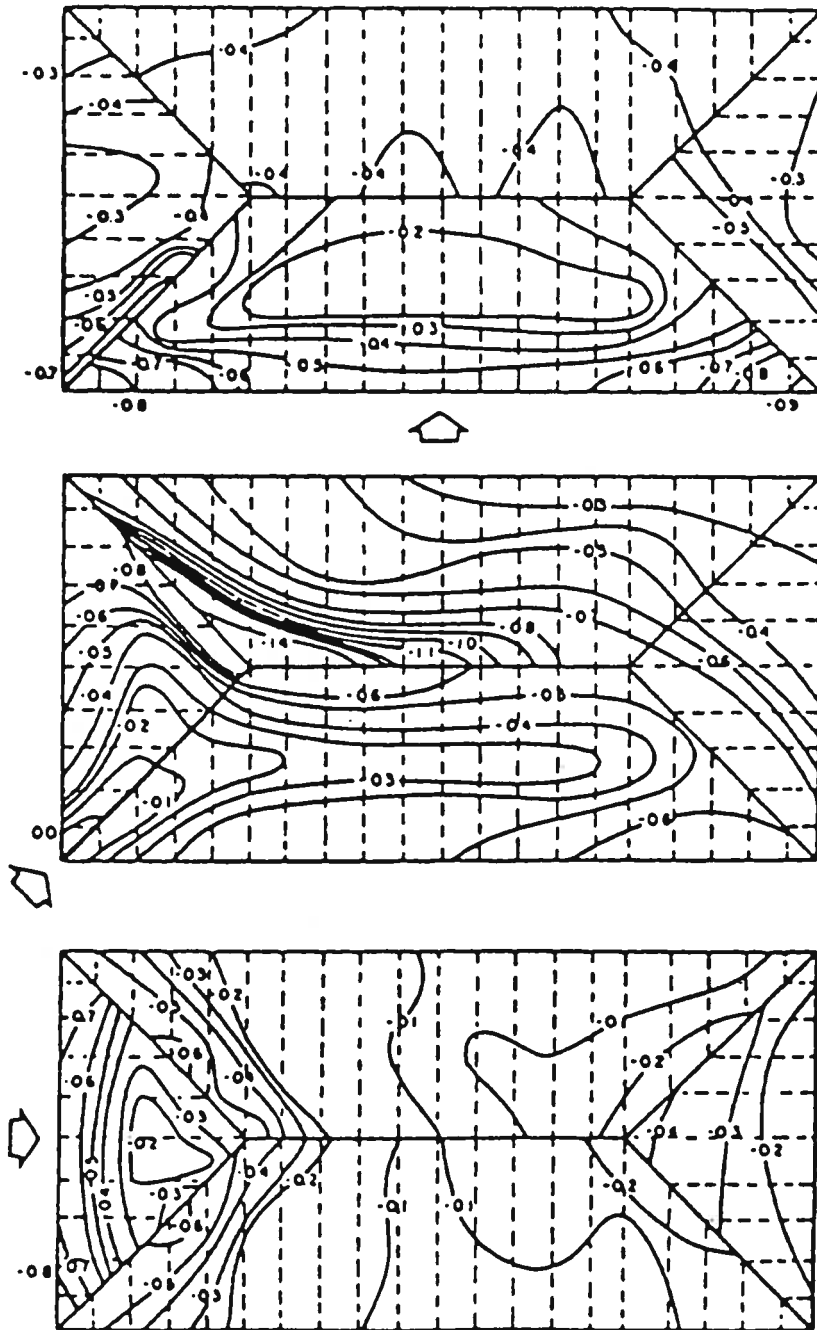


Fig. 10. Mean pressure coefficient distributions over a hip roof (Meecham [6]).

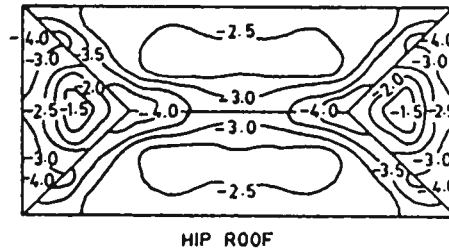


Fig. 11. Worst negative peak pressure coefficients over a hip roof – all azimuths (Meecham [6])

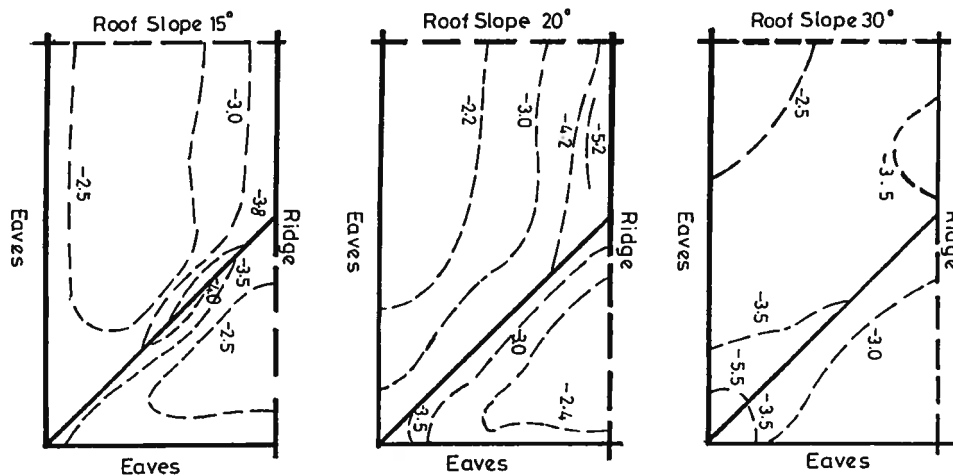


Fig. 12. Worst negative peak pressure coefficients over three hip roofs – all azimuths (present study).

quantity shown in Fig. 2, it is seen that both contour patterns and magnitudes from Meecham's work are, in general, similar to those obtained in this study for the 15° hip roof, but obviously not for the 30° hip roof.

Compared their contour of the worst negative peak pressure coefficient (Fig. 11) with the contour of the same quantity for the 15° hip roof shown in Fig. 6a, one can find that the contour patterns from the two sources are similar, but the contour magnitudes from the present study are lower than Meecham's results. Further efforts were then made to plot another set of contours of the worst negative peak pressure coefficient for all three tested hip roofs (Fig. 12). These new contours are based on the highest negative peak pressure in the five records rather than the average value of five records. It is seen now from Fig. 12 that the patterns of the new contours almost remain the same as those based on the average value of five records shown in Fig. 6a, but the magnitudes of the new contours are moderately larger than those shown in Fig. 6a. Furthermore, the new contour patterns and magnitudes for the 15° hip roof are now quite compatible with Meecham's counter shown in Fig. 11.

8. Conclusions

Three hip roofed building models of 15°, 20°, and 30° roof pitch, respectively, have been tested in a wind tunnel to investigate wind pressure distributions over hip roofs and the effect of roof pitch on roof pressures. The wind pressures measured on the hip roofs were compared with those on the gable roofs of otherwise similar geometry and the others' work on hip roofs.

The results showed that the effect of hip roof pitch on roof pressure was significant, particularly for peak suction. An increase in the pitch of a hip roof caused an increase in the worst peak suction. The 30° hip roof experienced the highest peak suction at roof corner among the three tested hip roofs. Compared with the gable roofs, the worst peak suction were much smaller on the hip roofs for 15° and 20° roof pitches. However, the worst peak suction on the hip and gable roofs were almost the same for 30° roof pitch. The worst peak suction on the three hip roofs occurred at different positions but possessed the same stochastic characteristics and exhibited only moderate deviations from the Gaussian density function. It has been also shown that the mean pressure contours for different wind directions and the worst negative peak pressure contour irrespective of wind direction obtained from this study were compatible with Meecham's work if the peak pressures of appropriate probability of occurrence were used.

Acknowledgements

The authors wish to thank Mr. McNealy, Senior Technical Officer at James Cook University, for his help in wind tunnel tests. Holmes and Meecham, whose work has been used as source, are gratefully acknowledged. Thanks are also due to the anonymous reviewers who made valuable comments on this study. This work was done when the first author was a Research Fellow at the Cyclone Testing Station of James Cook University, Australia.

References

- [1] A.G. Davenport, D. Surry, T. Stathopoulos, Wind loads on low rise buildings: Final report of Phase I and II, Boundary Layer Wind Tunnel Report BLWT-SS4, University of Western Ontario, Canada, 1978.
- [2] J.D. Holmes, Wind loads on low rise buildings – a review, CRISO, Division of Building Research, Highett, Victoria, Australia, 1993.
- [3] P.R. Sparks, J. Baker, J. Belville, D.C. Perry, Hurricane Elena Gulf Coast Aug 29–Sept. 2, Committee on Natural Disasters, Commission on Engineering and Technical Systems, Natural Research Council, USA, 1985.
- [4] Federal Emergency Management Agency, Building Performance: Hurricane Andrew in Florida—Observations, Recommendations, and Technical Guidance, Federal Insurance Administration, USA, 1992.
- [5] P.R. Sparks, M.L. Hessig, J.A. Murden, B.L. Sill, On the failure of single-story wood-frame houses in severe storms, J. Wind Eng. Ind. Aerodyn. 29 (1988) 245–252.

- [6] D. Meecham, D. Surry, A.G. Davenport, The magnitude and distribution of wind-induced pressures on hip and gable roofs, *J. Wind Eng. Ind. Aerodyn.* 38 (1991) 257–272.
- [7] J.D. Holmes, Wind pressures on houses with high pitched roofs, Wind Engineering Report 4/81, James Cook University, Townsville, Australia, 1981.
- [8] J.D. Holmes, Wind pressures and forces on tropical houses, Final Report of Project No. 17 of the Australian Housing Research Council, Melbourne, Australia, 1980.
- [9] Engineering Science Data Unit, Characteristics of atmospheric turbulence near the ground, part II: single point data for strong winds (neutral atmosphere), ESDU Data Item 85020, issued in 1985 and revised in 1993.
- [10] AS1170.2-SAA loading code, part 2: wind loads, Standard Association of Australia, NSW, Australia, 1989.
- [11] Y.L. Xu, Model and full-scale comparison of fatigue-related characteristics of wind pressures on the Texas Tech Buildings, *J. Wind Eng. Ind. Aerodyn.* 58 (1995) 147–173.